

# Preparation, spectral, X-ray powder diffraction and computational studies and genotoxic properties of new azo–azomethine metal chelates



Şirin Bitmez<sup>a</sup>, Koray Sayin<sup>b</sup>, Barış Avar<sup>c</sup>, Muhammet Köse<sup>a</sup>, Ahmet Kayraldız<sup>d</sup>, Mükerrerem Kurtoğlu<sup>a,\*</sup>

<sup>a</sup> Department of Chemistry, Kahramanmaraş Sutcu Imam University, 46100 Kahramanmaraş, Turkey

<sup>b</sup> Department of Chemistry, Cumhuriyet University, 58140 Sivas, Turkey

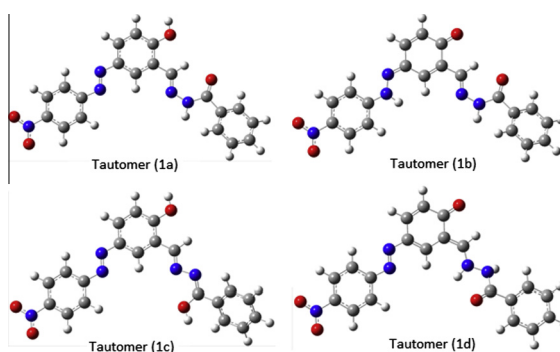
<sup>c</sup> Department of Metallurgy and Materials Engineering, Bulent Ecevit University, 67100 Zonguldak, Turkey

<sup>d</sup> Department of Biology, Kahramanmaraş Sutcu Imam University, 46100 Kahramanmaraş, Turkey

## HIGHLIGHTS

- A novel azo–azomethine ligand and its transition metal complexes were synthesized and characterized.
- The crystallinity of the azo–azomethine dye and its metal complexes were studied by X-ray powder diffraction.
- The geometrical parameters of the compounds are obtained as theoretically. The NLO properties of compounds are investigated.
- Finally, the ligand and its metal complexes are assessed for their genotoxicity.

## GRAPHICAL ABSTRACT



## ARTICLE INFO

### Article history:

Received 8 May 2014

Received in revised form 3 July 2014

Accepted 3 July 2014

Available online 22 July 2014

### Keywords:

Azo–azomethine

Spectroscopy

DFT studies

X-ray powder diffraction

Genotoxicity

Ames test

## ABSTRACT

A new tridentate azo–azomethine ligand, *N*-[2-hydroxy-5-[(4-nitrophenyl)diazanyl]phenyl]methylidene]benzohydrazidemonohydrate, (sbH·H<sub>2</sub>O) (**1**), is prepared by condensation of benzohydrazide and 2-hydroxy-5-[(4-nitrophenyl)diazanyl]benzaldehyde (**a**) with treatment of a solution of diazonium salt of *p*-nitroaniline and 2-hydroxybenzaldehyde in EtOH. The five coordination compounds, [Co(sb)<sub>2</sub>]-4H<sub>2</sub>O (**2**), [Ni(sb)<sub>2</sub>]-H<sub>2</sub>O (**3**), [Cu(sb)<sub>2</sub>]-4H<sub>2</sub>O (**4**), [Zn(sb)<sub>2</sub>]-H<sub>2</sub>O (**5**) and [Cd(sb)<sub>2</sub>]-H<sub>2</sub>O (**6**) are prepared by reacting the Co(II), Ni(II), Cu(II), Zn(II) and Cd(II) ions with the ligand. The structures of the compounds are elucidated from the elemental analyses data and spectroscopic studies. It is found the ligand acts as a tridentate bending through phenolic and carbonyl oxygens and nitrogen atom of the C=N– group similar to the most of salicylaldimines. Comparison of the infrared spectra of the ligand and its metal complexes confirm that azo–Schiff base behaves as a monobasic tridentate ligand towards the central metal ion with an ONO donor sequence. Upon complexation with the ligand, the Cd(II), and Zn(II) ions form monoclinic structures, while Co(II), Cu(II) and Ni(II) ions form orthorhombic structures. Quantum chemical calculations are performed on tautomers and its metal chelates by using DFT/B3LYP method. Most stable tautomer is determined as tautomer (**1a**). The geometrical parameters of its metal chelates are obtained as theoretically. The NLO properties of tautomer (**1a**) and its metal complexes are investigated. Finally, the ligand and its metal complexes are assessed for their genotoxicity.

© 2014 Elsevier B.V. All rights reserved.

\* Corresponding author. Tel.: +90 344 280 1450; fax: +90 344 280 1352.

E-mail addresses: [mkurtoğlu@ksu.edu.tr](mailto:mkurtoğlu@ksu.edu.tr), [kurtoğlu01@gmail.com](mailto:kurtoğlu01@gmail.com) (M. Kurtoğlu).

## Introduction

Azo-Schiff bases play an important role in inorganic chemistry as they easily form stable complexes with most transition metal ions such as cobalt(II), nickel(II) and copper(II). The development of the field of bioinorganic chemistry has increased the interest in Schiff base complexes, since it has been recognized that many of these complexes may serve as models for biologically important species [1–3]. Schiff base ligands are well known for their wide range of applications in pharmaceutical and industrial fields [4–6]. Transition metal complexes of polydentate Schiff base ligand have great applicabilities in catalysis and material chemistry [7]. Moreover, the hydrazone group plays an important role for the antimicrobial activity and possesses interesting antibacterial, anti-fungal [8,9], anti-tuberculosis activities [10,11]. These groups of compounds are important class of ligands which present in numerous physiological and biological applications as antitumour agents, insecticides, anticoagulants, anticonvulsant, anti-inflammatory, analgesic, antioxidants, antiplatelet and plant growth regulators [12–16]. These properties of the hydrazones are attributed to the formation of stable metal complexes with some metals which catalyze physiological processes. Their metal complexes, have also found applications in various chemical processes like nonlinear optics, sensors, medicine [17].

Recently, azo-Schiff bases and their metal complexes were reported by our group [18–20]. In view of the versatile importance of azo-azomethines, hydrazones and their metal complexes, we herein describe the preparation and identification of Co(II), Ni(II), Cu(II), Zn(II) and Cd(II) metal complexes of *N*'-[(2-hydroxy-5-[(4-nitrophenyl)diazenyl]phenyl)methylidene]benzohydrazidemonohydrate, sbH. The chemical equations concerning the formation of the sbH ligand represented as Scheme 1. The newly synthesized azo-azomethine ligand and its metal chelates were characterized by their IR, electronic, and elemental analyses data. Finally, the

ligand sbH and its Co(II), Ni(II), Cu(II), Zn(II) and Cd(II) metal complexes were tested for their genotoxic properties.

## Experimental

### Reagents

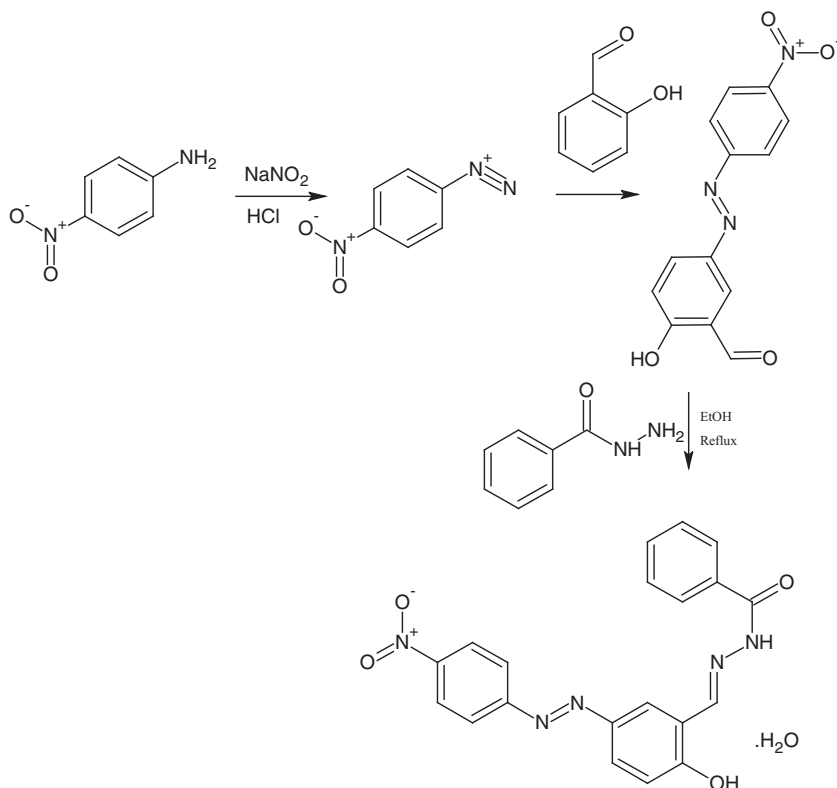
All reagents and solvents used were supplied by Merck chemical company and were used without further purification.

### Physical measurements

<sup>1</sup>H NMR spectrum of the ligand was obtained in deuterated DMSO as solvent on a Bruker FT-NMR AC-400 (300 MHz) spectrometer. All chemical shifts are reported in  $\delta$  (ppm) relative to the tetramethylsilane as internal standard. Carbon, hydrogen and nitrogen elemental analyses were performed with a model LECO CHNS 932 elemental analyzer. IR spectra were obtained using KBr discs (4000–400  $\text{cm}^{-1}$ ) on a Perkin Elmer FT-IR spectrophotometer. The UV-Vis spectra of DMSO solutions in the 200–800 nm range were measured on a T80+ UV-Vis. Spectrometer PG Instruments LTD spectrometer. X-ray powder diffraction analysis was performed by PANalytical X'Pert PRO instrument with Cu K $\alpha$  radiation (wavelength 0.154 nm) operating at 40 kV and 30 mA. Measurements were scanned for diffraction angles ( $2\theta$ ) ranging from 5° to 50° with a step size of 0.02° and a time per step of 1 s. Melting points were obtained with a Electrothermal LDT 9200 Apparatus in open capillaries.

### Synthesis of 2-hydroxy-5-[(4-nitrophenyl)diazenyl]benzaldehyde, (**a**)

The azo-coupled salicylaldehyde was synthesized using the known coupling methods [18]. A 1.22 g (10 mmol) of salicylaldehyde was dissolved in distilled water (30 mL) containing 0.7 g



**Scheme 1.** The synthesis reaction of *N*'-[(2-hydroxy-5-[(4-nitrophenyl)diazenyl]phenyl)methylidene]benzohydrazidemonohydrate (sbH·H<sub>2</sub>O).

(8.8 mmol) of sodium hydroxide and 40 mmol of sodium carbonate during the period of 30 min at 0 °C. The resulted solution was added slowly to the solution of diazonium chloride of 1.38 g (10 mmol) *p*-nitroaniline in water at 0–5 °C. The reaction mixture was stirred for 1 h at 0 °C and, then allowed to warm slowly to the room temperature. The product was collected by filtration and washed with a 100 mL of NaCl solution (10%) under vacuum. The obtained yellowish orange solid was dried under vacuum at 80 °C overnight. Yield, 85%, m.p. 182–183 °C; orange powder. <sup>1</sup>H NMR (d<sub>6</sub>-DMSO, δppm). 10.36 (s, –CHO), 8.01–7.98 (t, Ar–H), 7.26–7.23 (d, Ar–H) 7.14–7.11 (d, Ar–H), 11.41 (s, Ar–OH). IR(KBr, cm<sup>-1</sup>): 3104 (O–H), 2903 (Ar–C–H), 1657 (C=O), 1104 (N–O).

*Synthesis of N'-[2-hydroxy-5-[(4-nitrophenyl)diazanyl]phenyl]methylidene]benzohydrazidemonohydrate (sbH-H<sub>2</sub>O) (1)*

A hot solution of benzohydrazide (0.865 g, 6.378 mmol) in 25 mL EtOH was mixed with hot solution (60 °C) of 2-hydroxy-5-[(4-nitrophenyl)diazanyl]benzaldehyde (1.73 g, 6.378 mmol) in the same solvent (30 mL) and the reaction mixture was stirred magnetically under reflux for 2 h. The formed orange-yellow product was dissolved in 25 mL EtOH and left for crystallization at room temperature for a day. Then yellow product was collected, washed with cold EtOH and dried in a vacuum. Yield, 60%, m.p. 291–292 °C. Anal. Calcd. for C<sub>20</sub>H<sub>17</sub>N<sub>5</sub>O<sub>5</sub> (407.38 g/mol): C, 58.97; H, 4.21; N, 17.19. Found: C, 58.37; H, 4.075; N, 16.69%. IR (KBr, cm<sup>-1</sup>): 3400 (O–H), 3105 (Ar–C–H), 1650 (C=O), 1510 (C=N), 1489 (N=N), 1185 (C–O), 1070 (N–O).

*Synthesis of bis{N'-[2-hydroxy-5-[(4-nitrophenyl)diazanyl]phenyl]methylidene]benzohydrazide}cobalt(II)tetrahydrate, [Co(sb)<sub>2</sub>]-4H<sub>2</sub>O (2)*

A solution of CoCl<sub>2</sub>·6H<sub>2</sub>O (0.076 g, 0.32 mmol) in 20 mL of EtOH was added to a magnetically stirred 15 mL EtOH solution containing of the ligand (0.25 g, 0.64 mmol) at 70 °C. The obtained solution was left at room temperature. The cobalt(II) complex was obtained as dark red precipitates. The reddish brown product was filtered, washed with EtOH, and then dried under the vacuum. Yield, 82%, decomposed at >300 °C; reddish brown powder. Anal. Calcd. for C<sub>40</sub>H<sub>36</sub>N<sub>10</sub>CoO<sub>12</sub>. (837.66 g/mol): C, 52.93; H, 4.00; N, 15.43. Found: C, 53.13; H, 3.456; N, 15.48%. IR (KBr): 3420 (O–H), 3100 (Ar–C–H), 1618 (C=O), 1518 (C=N), 1485 (N=N), 1090 (N–O), 625 (Co–O), 515 (Co–N).

*Synthesis of bis{N'-[2-hydroxy-5-[(4-nitrophenyl)diazanyl]phenyl]methylidene]benzohydrazide}nickel(II)monohydrate, [Ni(sb)<sub>2</sub>]-H<sub>2</sub>O (3)*

0.25 g (0.64 mmol) of sbH-H<sub>2</sub>O ligand was dissolved in 20 mL EtOH at room temperature. A solution of 0.076 g (0.32 mmol) NiCl<sub>2</sub>·6H<sub>2</sub>O (10 mL) was added dropwise into 20 mL of EtOH with continuous stirring. The stirred mixture was then heated to the reflux temperature and maintained at this temperature for 2 h. Then, the mixture was evaporated to a volume of 15 mL in vacuum and left to cool to the room temperature. The product was filtered in vacuum and washed with a small amount of cold ethanol. The product was recrystallized from EtOH and dried at room temperature. Yield, 76%, decomposed at >300 °C; reddish brown powder. Anal. Calcd. for C<sub>40</sub>H<sub>30</sub>N<sub>10</sub>NiO<sub>9</sub> (853.42 g/mol): C, 56.29; H, 3.54; N, 16.87. Found: C, 56.18; H, 3.36; N, 16.07%. IR (KBr, cm<sup>-1</sup>): 3415 (O–H), 3115 (Ar–C–H), 1615 (C=O), 1520 (C=N), 1475 (N=N), 1092 (N–O), 690 (Ni–O), 515 (Ni–N).

*Synthesis of bis{N'-[2-hydroxy-5-[(4-nitrophenyl)diazanyl]phenyl]methylidene]benzohydrazide}copper(II)tetrahydrate, [Cu(sb)<sub>2</sub>]-4H<sub>2</sub>O (4)*

A solution of CuCl<sub>2</sub>·2H<sub>2</sub>O (0.055 g, 0.32 mmol) in EtOH (15 mL) was added to the sbH-H<sub>2</sub>O ligand solution (0.25 g, 0.64 mmol) in EtOH (30 mL), and the mixture was refluxed with stirring for 2 h. After stripping off the excess solvent under reduced pressure, a brown product was obtained. Yield, 73%, decomposed at >300 °C; brown powder. Anal. Calcd. for C<sub>40</sub>H<sub>36</sub>CuN<sub>10</sub>O<sub>12</sub> (840.25 g/mol): C, 52.66; H, 3.36; N, 15.35. Found: C, 52.43; H, 3.32; N, 15.04%. IR (KBr, cm<sup>-1</sup>): 3425 (O–H), 3080 (Ar–C–H), 1610 (C=O), 1517 (C=N), 1480 (N=N), 1095 (N–O), 730 (Cu–O), 518 (Cu–N).

*Synthesis of bis{N'-[2-hydroxy-5-[(4-nitrophenyl)diazanyl]phenyl]methylidene]benzohydrazide}zinc(II)monohydrate, [Zn(sb)<sub>2</sub>]-H<sub>2</sub>O (5)*

This compound was prepared by the addition of Zn(CH<sub>3</sub>COO)<sub>2</sub>·2H<sub>2</sub>O (0.07 g, 0.32 mmol) in EtOH (15 mL) to a refluxing mixture of the ligand sbH-H<sub>2</sub>O (0.25 g (0.64 mmol) in EtOH (30 mL). The red compound was separated out on filtration, washed with cold EtOH and dried *in vacuo*. Yield, 85%, decomposed at >300 °C; red powder. Anal. Calcd for C<sub>40</sub>H<sub>30</sub>N<sub>10</sub>ZnO<sub>9</sub> (860.14 g/mol): C, 55.85; H, 3.52; N, 16.74. Found: C, 55.85; H, 3.335; N, 16.04%. IR (KBr): 3420 (O–H), 3085 (Ar–C–H), 1615 (C=O), 1522 (C=N), 1485 (N=N), 1090 (N–O), 615 (Zn–O), 523 (Zn–N).

*Synthesis of bis{N'-[2-hydroxy-5-[(4-nitrophenyl)diazanyl]phenyl]methylidene]benzohydrazide}cadmium(II)monohydrate, [Cd(sb)<sub>2</sub>]-H<sub>2</sub>O (6)*

To a solution of the sbH-H<sub>2</sub>O ligand (0.25 g, 0.64 mmol) in EtOH (30 mL) was added, a solution of Cd(CH<sub>3</sub>COO)<sub>2</sub>·2H<sub>2</sub>O (0.086 g, 0.32 mmol) in EtOH and the resulting solution was boiled under reflux for 2 h. The precipitated red complex was filtered, washed with cold EtOH and dried *in vacuo*. Yield, 78%, decomposed at >300 °C; red powder. Anal. Calcd. for C<sub>40</sub>H<sub>30</sub>N<sub>10</sub>CdO<sub>9</sub>. (907.14 g/mol): C, 52.96; H, 3.33; N, 15.44. Found: C, 52.85; H, 3.16; N, 15.44%. IR (KBr): 3420 (O–H), 3100 (Ar–C–H), 1610 (C=O), 1533 (C=N), 1480 (N=N), 1095 (N–O), 625 (Cd–O), 520 (Cd–N).

*Computational method*

Gaussian 09 package programs were used for all calculations [21,22]. Density functional theory (DFT/B3LYP) method with 6-31++G(d,p) and LANL2DZ basis sets was used for obtaining the optimized structure of the possible tautomers and its transition metal complexes, respectively. For organic molecules, basis sets which contain diffuse and polar functions give the most appropriate results. Therefore, 6-31++G(d,p) was selected for tautomers. LANL2DZ basis set has been used for various complexes in many computational studies. The calculated vibrational frequencies were scaled by 0.95 [23] and 0.9614 [24] for B3LYP/6-31++G(d,p) and B3LYP/LANL2DZ, respectively.

*Ames test*

*The chemicals used in the experiment*

All the test substances (sbH-H<sub>2</sub>O, [Co(sb)<sub>2</sub>]-4H<sub>2</sub>O, [Ni(sb)<sub>2</sub>]-H<sub>2</sub>O, [Cu(sb)<sub>2</sub>]-4H<sub>2</sub>O, [Zn(sb)<sub>2</sub>]-H<sub>2</sub>O and [Cd(sb)<sub>2</sub>]-H<sub>2</sub>O) were suspended in DMSO with the final concentrations of 0.80, 0.40, 0.20, 0.10 and 0.05 mg/plate, for testing mutagenicity. Mutagenicity test tablets containing nicotinamide adenine dinucleotide phosphate (NADP) and glucose-6-phosphate were purchased from Boehringer Mannheim Biochemicals (Germany). DMSO (D8418), 1-histidin (H8125), d-biotin (B4501), ampicillin (A6140), sodium azide (SA,

S2002) and 2-aminofluorene (2-AF, A9031) were purchased from Aldrich; agar (7178) was purchased from Aquamedia; nutrient broth (NB, B241116) was purchased from Oxoid; 3-methylcolanthrene (200-276-4) was purchased from Oekanal. In this study 2-AF (dissolved in DMSO), NPD (4-nitro-*o*-phenylene diamine) (dissolved in DMSO) and SA (dissolved in bidistilled water) were used as positive controls [25].

#### Preparations of S9 mix

The albino male rats (*Rattus norvegicus* var. albinos) weighting 200 g were pre-treated with 80 mg/kg concentration of 3-methylcolanthrene (dissolved in sunflower oil) for 5 days and the S9 fraction and S9 mix were prepared following the procedure of Maron and Ames [26]. S9 fraction (microsome fraction) was prepared and immediately distributed to small plastic tubes at 1 mL quantity and then stored at  $-35^{\circ}\text{C}$ . The S9 mix was prepared fresh for each mutagenicity assay. For preparation of S9 mix, one S9 tablet dissolved in 18 mL of sterile bidistilled water supplemented with 2 mL of microsome fraction; 0.5 mL of S9 mix was used for each plate. S9 mix contains microsome fraction, NADP, G-6-P and other salt solutions [26,27].

#### Bacterial strains

Histidin deficient ( $\text{his}^{-}$ ) tester strains TA98 and TA100 of *Salmonella typhimurium* were kindly provided by J.L. Swezey, Curator, ARS Patent Culture Collection, Microbial Genomics and Bioprocessing Research Unit, North University Street, Peoria, Illinois 61604, USA. The TA100 strain is used for the detection of base-pair substitution mutagens and TA98 strain is used for the detection of frame-shift mutagens. Each strain before use in the assay was checked for the presence of strain-specific marker as described Maron and Ames [26].

#### Mutagenicity assay

Standard procedure of plate incorporation assay was carried out by using TA98 and TA100 strains for examining the frameshift mutagens and base-pair substitution mutagens, respectively. Using both strains, the Ames test was performed with metabolic activation (+S9 mix) to obtain a first approximation of mammalian metabolism, and without metabolic activation (–S9 mix). The assay was carried out according to published paper [28]. TA98 and TA100 strains were exposed to a range of concentrations of each test substance in a soft agar overlay. The number of revertants observed in each concentration of test substances and in spontaneous control were scored.

#### Statistical significance

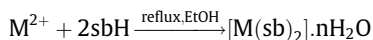
The observed differences between the test substances and control groups (spontaneous control and positive control) were analyzed by *t*-test. Regression and correlation tests were used for dose-response relationships.

## Results and discussion

#### Synthesis

The results of the elemental analyses of the ligand and its complexes are in agreement with the chemical formulae. The azo-Schiff base ligand  $N'-[2\text{-hydroxy-5-}[(4\text{-nitrophenyl)diazenyl]phenyl]methylidene]benzohydrazidemonohydrate$ ,  $\text{sbH}\cdot\text{H}_2\text{O}$  was synthesized in good yields in EtOH. The ligand is stable at room temperature and soluble in common organic solvents such as DMSO, DMF, EtOH and MeOH. The complexes are also stable at room temperature. Based on the elemental analyses, spectroscopic characterization, these mononuclear complexes are presumed to have the coordination

environment shown in Fig. 1. Single crystals of the compounds could not be isolated from any organic solution, thus no definite structures can be described. However, the analytical and spectroscopic data enables us to predict possible structures as shown in Scheme 2 and Figs. 1 and 2.



$\text{sbH}\cdot\text{H}_2\text{O}: N'-[2\text{-hydroxy-5-}[(4\text{-nitrophenyl)diazenyl]phenyl]methylidene]benzohydrazide$   $M = \text{Co(II)}$  ( $n = 4$ ),  $\text{Ni(II)}$  ( $n = 1$ ),  $\text{Cu(II)}$  ( $n = 4$ ),  $\text{Zn(II)}$  ( $n = 1$ ),  $\text{Cd(II)}$  ( $n = 1$ )

#### $^1\text{H}$ NMR spectrum of the ligand

Evidence of the bonding mode of sbH was also provided by the  $^1\text{H}$  NMR spectrum of the azo-azomethine ligand. The  $^1\text{H}$  NMR spectrum of the compound was obtained in deuterated dimethylsulfoxide solution at room temperature using TMS as an internal standard. The  $^1\text{H}$  NMR spectrum of the sbH ligand was given in Fig. 1, and the chemical shifts of the different types of protons in the  $^1\text{H}$  NMR spectrum of sbH·H<sub>2</sub>O ligand are also listed in Table 1. The tautomeric azo-imine form of the sbH azo-azomethine dye is indicated by  $^1\text{H}$  NMR spectroscopy. The  $^1\text{H}$  NMR spectrum of sbH ligand showed a singlet signal at  $\delta$  12.25 ppm, which was attributed to phenolic –OH proton (7a) [29]. The proton of the amide group (–CO–NH–N=C) of the ligand (10a) appears also as a singlet at 12.01 ppm. It is well known that hydrogen bonded OH proton resonance appears at a lower field than that of NH proton resonance [30]. Therefore, it may be concluded that the dye exists in the azo-imine tautomeric form in DMSO solution. The ligand also showed one singlet at  $\delta$  8.80 ppm which was attributed to the azomethine proton (8a) [31,32]. The  $^1\text{H}$  NMR spectrum of the ligand revealed a singlet at  $\delta$  8.34 ppm, corresponding to proton of aromatic structure linked nitrophenylazo group (3a). The spectrum of sbH showed peaks at  $\delta$  8.43 (*d*, 17a and 19a),  $\delta$ 8.08 (*d*, 16a and 20a),  $\delta$ 7.97 (*d*, 22a and 26a),  $\delta$ 7.96 (*d*, 5a),  $\delta$ 7.63 (*t*, 23a and 25a),  $\delta$ 7.55 (*t*, 24a) and  $\delta$ 7.07 (*d*, 6a) which are attributed to aromatic hydrogens. Additionally, there is also water protons of the solvent ( $\text{d}_6\text{-DMSO}$ ) and the sample observed at  $\delta$ 3.33 ppm [33]. The presence of water in the structure was also confirmed by IR spectroscopy and elemental analysis. These results are in agreement with the literature [18].

#### IR spectra

The IR spectra of the tridentate sbH·H<sub>2</sub>O ligand and its complexes have been studied in order to characterize their structures. The characteristic IR data of the azo-azomethine ligand and its metal complexes are given in the experimental section. The comparison of IR spectra of the compounds imply that the ligand, sbH, is monobasic tridentate in nature with carbonyl-oxygen, azomethine-nitrogen and phenolic-oxygen as the coordination sites. In the ligand and complexes spectra, both ligand and complexes exhibit bands at  $3400\text{--}3425\text{ cm}^{-1}$  and  $3085\text{--}3115\text{ cm}^{-1}$  that are assignable to  $\nu(\text{OH})$  and  $\nu(\text{Ar-C-H})$  [31,34]. Disappearance of the broad band due to H-bonded phenolic O–H stretching in the spectra of metal complexes confirmed the coordination of phenolic oxygen atom to metal ions. The broad band centered at  $3200\text{--}3275\text{ cm}^{-1}$  in the free ligand can be assigned to the amide –N–H stretching, which remains unaltered in the complexes [35]. This suggests that the non-participation of amide NH group in coordination. The band at  $1545\text{ cm}^{-1}$  is due to the vibration of the azomethine group (–CH=N–) of the ligand [36]. This band in the metal complexes shifted to higher frequencies as a result of coordination of the azomethine nitrogen atom to the metal ion. The C=O observed at  $1650\text{ cm}^{-1}$  in the spectrum of the ligand showed a

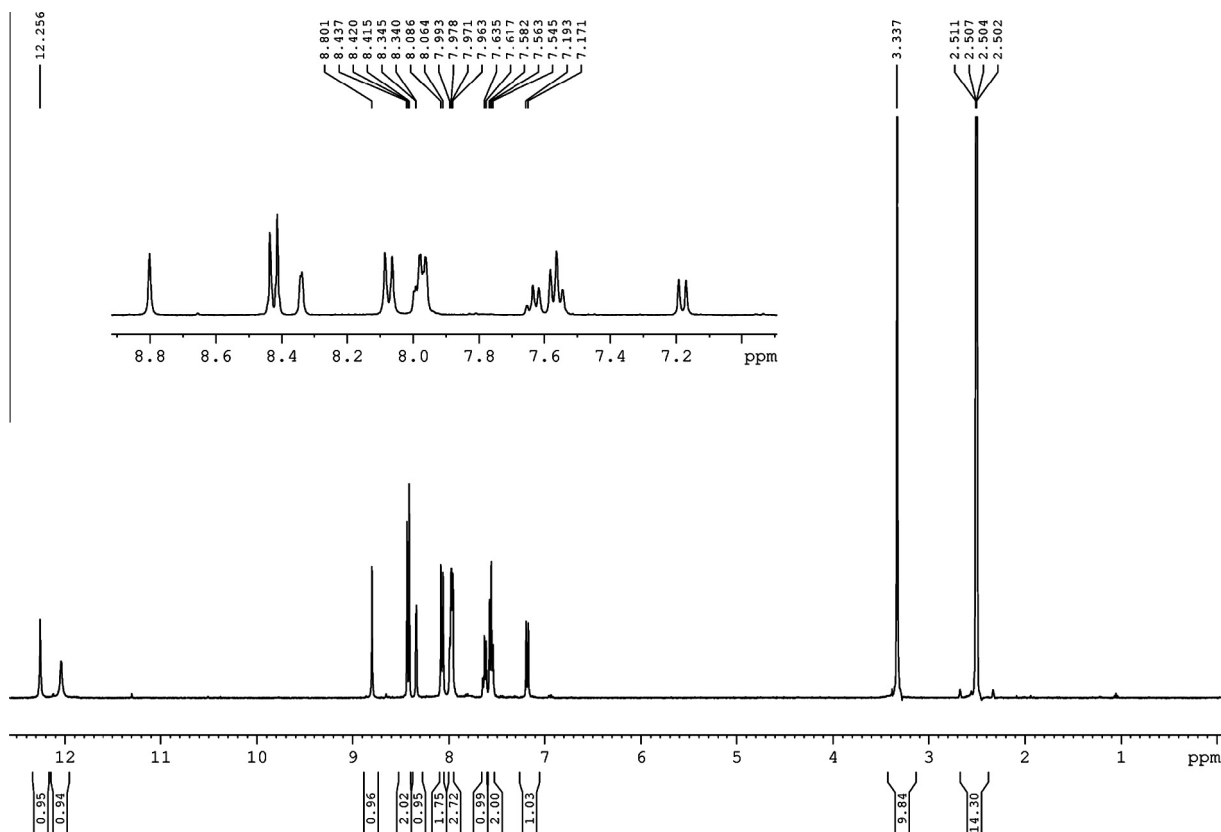
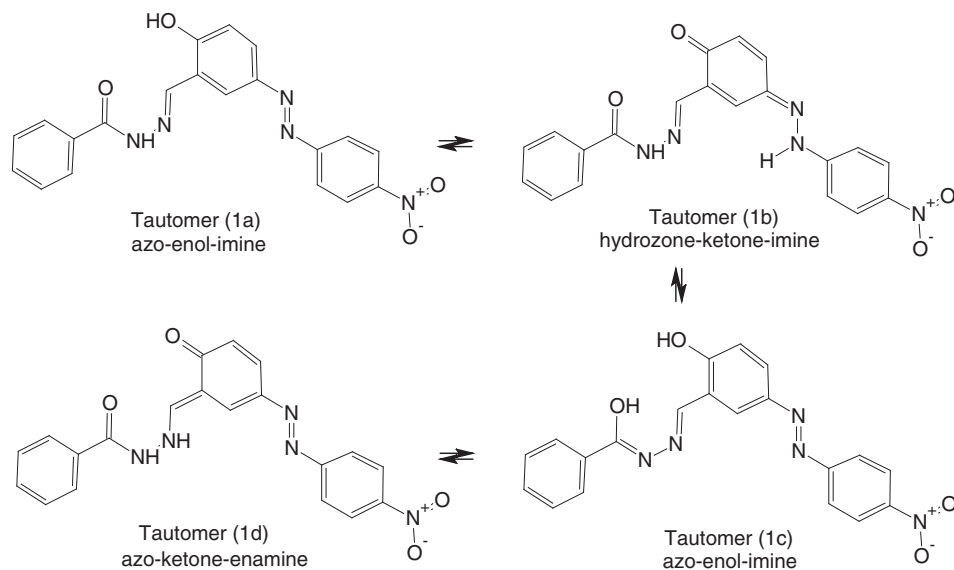


Fig. 1. The  $^1\text{H}$  NMR spectrum of the azo-azomethine (sbH) ligand in  $\text{d}_6$ -DMSO.

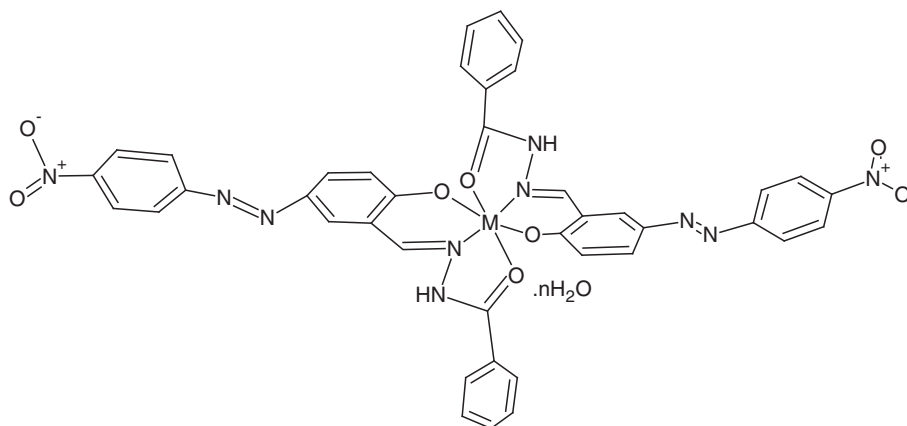


Scheme 2. Tautomeric forms of the sbH ligand.

downward shift to  $1618\text{--}1610\text{ cm}^{-1}$  in all the complexes indicating the coordination through the carbonyl oxygen [37].

Hence, from the infrared spectroscopic data, it is inferred that azomethine nitrogen, carbonyl and phenolic oxygen atoms are involved in the coordination with transition metal ion in all complexes. The peak appearing in the region  $1475\text{--}1489\text{ cm}^{-1}$  is attributed to ( $\text{--N=N--}$  stretching vibration) [34,38]. The absorption

bands observed at  $1070\text{--}1095\text{ cm}^{-1}$  are assigned to N–O stretching vibrations of the dye and its metal chelates. In addition to the above bands all the complexes display the new bands in the far infrared region  $615\text{--}730$  and  $515\text{--}520\text{ cm}^{-1}$  were assigned to  $\nu(\text{M--O})$  and  $\nu(\text{M--N})$  vibrations, respectively [39]. These data are in agreement with those previously reported for similar compounds.



M = Co(II) (m = 4), Ni(II) (n = 1), Cu(II) (n = 4), Zn(II) (n = 1), Cd(II) (n = 1)

Fig. 2. The proposed structure of the metal complexes.

**Table 1**  
The  $^1\text{H}$  NMR data (ppm) of the azo-azomethine (sbH $\cdot$ H $_2$ O) ligand in  $\text{d}_6$ -DMSO.

Chemical shifts, $\delta_{\text{TMS}}$ (ppm)	Assignments <sup>a</sup>	J (Hz)
12.25	[s, 1H] (7a)	–
12.01	[s, 1H] (10a)	–
8.80	[s, 1H] (8a)	–
8.43	[d, 2H] (17a, 19a)	9.11
8.34	[s, 1H] (3a)	–
8.08	[d, 2H] (16a, 20a)	8.87
7.97	[d, 2H] (22a, 26a)	7.05
7.96	[d, 1H] (5a)	7.18
7.63	[t, 2H] (23a, 25a)	7.32
7.55	[t, 1H] (24a)	7.59
7.07	[d, 1H] (6a)	8.85
3.33	[water-H]	–
2.51	[DMSO-H]	–

<sup>a</sup> s: singlet; d: doublet and t: triplet.

### Electronic spectra

The electronic absorption spectra of the azo-azomethine ligand and its complexes (I–VI) were obtained in  $10^{-3}$  M DMSO solutions at room temperature. The UV–Vis spectral data of the synthesized

ligand and its metal complexes are summarized in Table 2. The UV–Vis spectra of the azo-Schiff Base ligand containing  $-\text{N}=\text{N}-$  chromophore and its metal complexes in DMSO showed two or three absorption bands between 235 and 340 nm, as shown in Figs. 3 and 4, respectively. The first band is referred to the  $\pi \rightarrow \pi^*$  transitions of the aromatic, azomethine or  $-\text{N}=\text{N}-$  groups. The second band ranged 320–340 nm is due to  $n \rightarrow \pi^*$  transition in the azomethine system [40]. The longer wavelength band at 395–405 nm can be assigned to  $n \rightarrow \pi^*$  transition in the  $-\text{N}=\text{N}-$  chromophore group of the ligand and its metal chelates [41]. The bands at 500 nm and 535 nm in the spectra of the Zn(II) and Cd(II) complexes, respectively can be also assigned to an intra-molecular charge transfer interaction. In addition to that, the electronic spectra of the Co(II), Ni(II) and Cu(II) complexes exhibited a band at 510, 530 and 487 nm, respectively. These bands are assigned to  $d-d$  transition in the complexes. These bands are characteristic of octahedral complexes.

### Computational studies

#### The optimized structures and vibrational frequencies of tautomers

The possible tautomers of the synthesized azo-azomethine dye are optimized at B3LYP/6-31++G(d,p) level in vacuum. The optimized structures of these tautomers are represented in Fig. 5. These tautomers exist together in solution media but one of these tautomers is the most stable. The most stable tautomer can be determined as theoretically by taking into account total energy ( $E_{\text{Total}}$ ), enthalpy (H) and Gibbs free energy ( $G^\circ$ ) values which are thermochemical parameters. Total energy, enthalpy and Gibbs free energy include the zero-point energy and thermal corrections. The mentioned parameters are represented in Table 3. According to the  $E_{\text{Total}}$ , H and  $G^\circ$ , ranking of tautomer stability should be as follow:

**Table 2**  
UV–Vis. (nm) data of the synthesized ligand and its metal complexes in DMSO.

Compound	Absorption		$\lambda_{\text{max}}$ (nm)	
	$\pi \rightarrow \pi^*$	$n \rightarrow \pi^*$	$n \rightarrow \pi^*/\text{CT}$	$d \rightarrow d$
(1) sbH $\cdot$ H $_2$ O	235	320	405	–
(2) [Co(sb) $_2$ ] $\cdot$ 4H $_2$ O	240	334	400	–510
(3) [Ni(sb) $_2$ ] $\cdot$ H $_2$ O	240	320	400	530
(4) [Cu(sb) $_2$ ] $\cdot$ 4H $_2$ O	240	320	395	487
(5) [Zn(sb) $_2$ ] $\cdot$ H $_2$ O	240	320	395/500	–
(6) [Cd(sb) $_2$ ] $\cdot$ H $_2$ O	240	320	395/535	–

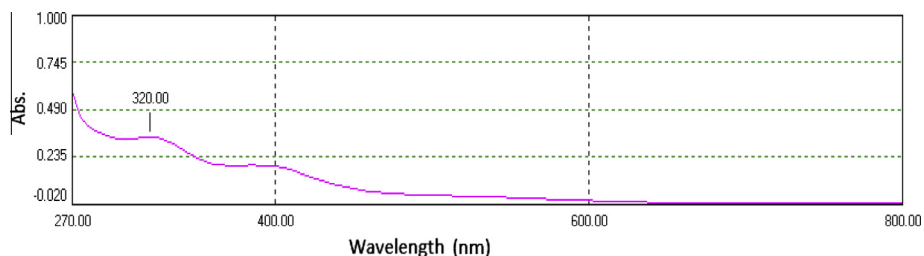


Fig. 3. The UV-Vis. spectrum of the ligand in DMSO.

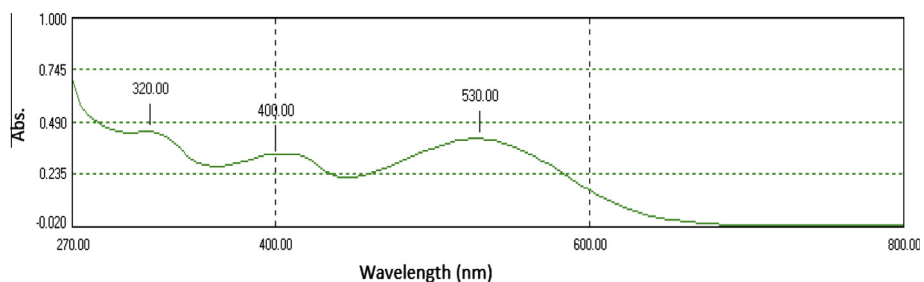


Fig. 4. The UV-Vis. spectrum of the Ni(II) complex in DMSO.

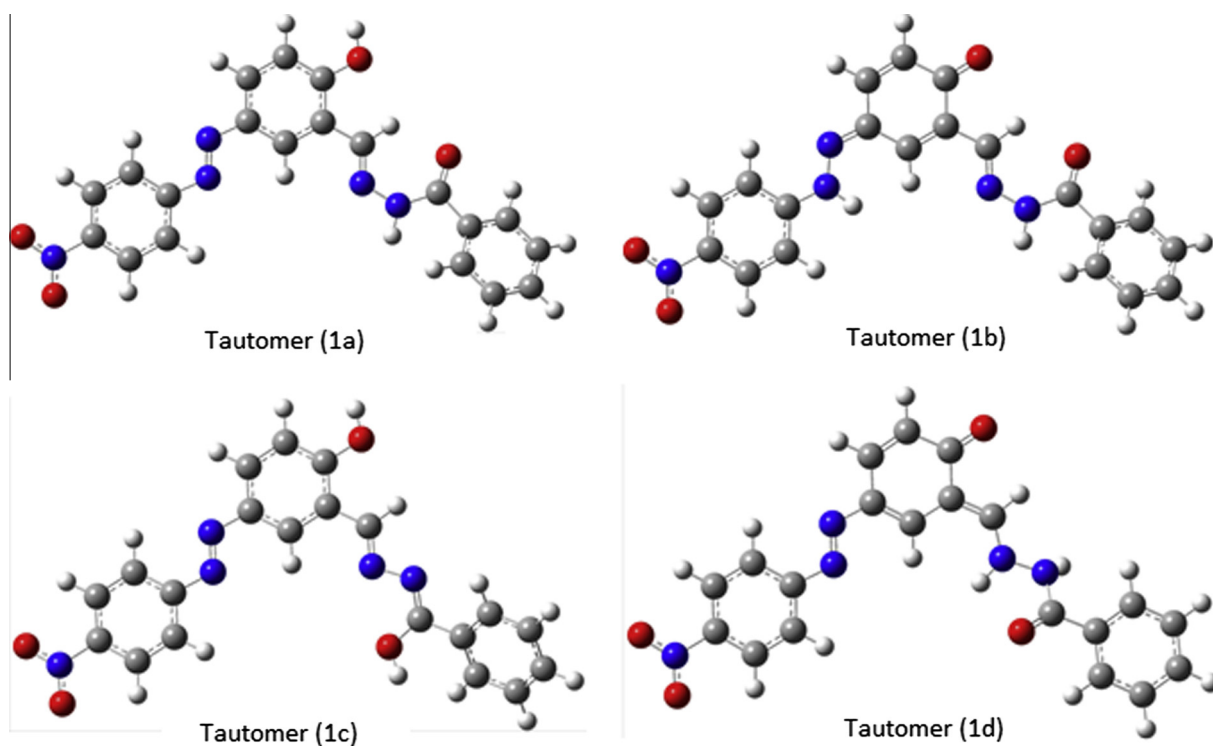


Fig. 5. Optimized structures of tautomers at B3LYP/6-31++G(d,p) level of theory in gas phase.

Table 3

Calculated thermochemical parameters (a.u.) of tautomers.

Tautomers	$E_{\text{Total}}$	$H$	$G^\circ$
Tautomer (1a)	-1345.387474	-1345.386529	-1345.471405
Tautomer (1b)	-1345.379271	-1345.378326	-1345.463065
Tautomer (1c)	-1345.370056	-1345.369111	-1345.455051
Tautomer (1d)	-1345.369709	-1345.368764	-1345.454677

(1a) > (1b) > (1c) > (1d). The tautomer with the lowest energy has the most stable structure. According to this ranking, the most stable tautomer is tautomer (1a). Infrared spectrum of the tautomer (1a) is calculated and the vibration frequencies are scaled by using

Table 4

The calculated quantum chemical parameters at B3LYP/6-31++G(d,p) level.

Labels <sup>a</sup>	$P_k(N+1)$	$P_k$	$P_k(N-1)$	$f_k^+$	$s$ (eV <sup>-1</sup> )
N1	7.33995	7.44731	7.44414	-0.10736	0.00179
N2	7.20424	7.31265	7.26149	-0.10841	0.02892
O1	8.52528	8.61746	8.59768	-0.09218	0.01118
O2	8.31699	8.70903	8.45201	-0.39204	0.14531
O3	8.27064	8.42426	8.37641	-0.15362	0.02705
O4	8.28935	8.42537	8.37739	-0.13602	0.02713

<sup>a</sup> Atomic labels are defined in Fig. 2.

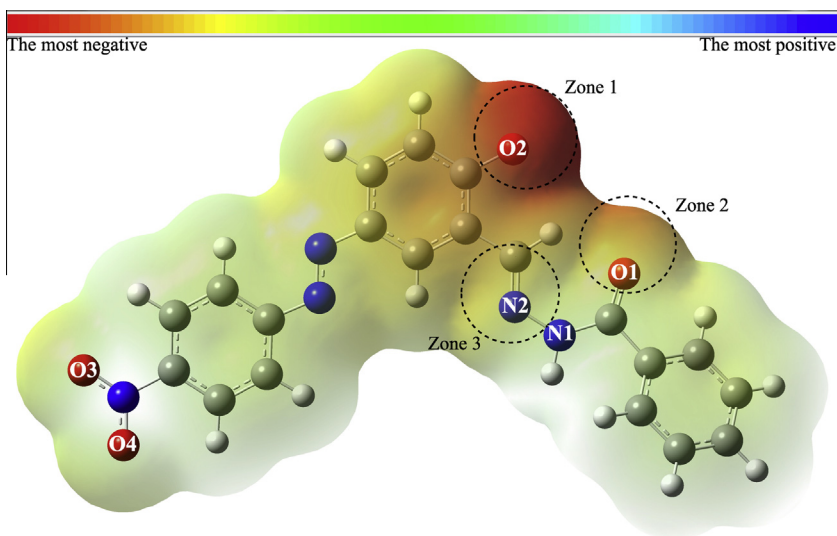


Fig. 6. The MEP diagram of deprotonated form of tautomer (1) at B3LYP/LANL2DZ level.

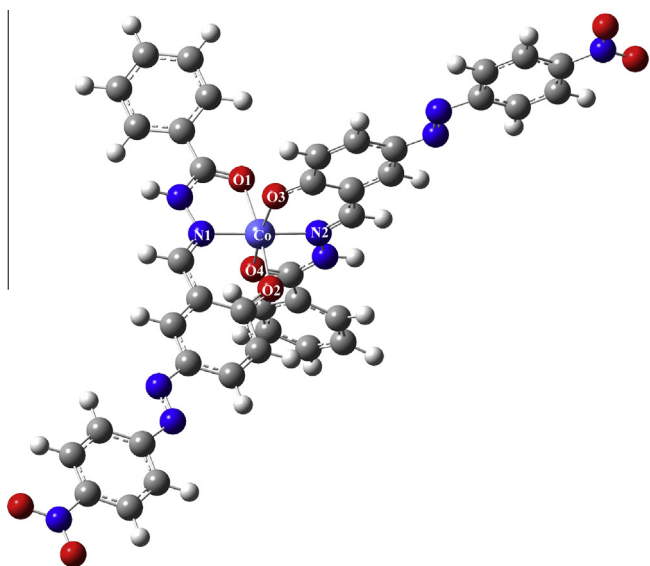


Fig. 7. Optimized structure of  $[\text{Co}(\text{sb})_2]$  complex at B3LYP/LANL2DZ level in gas phase.

0.95. Some vibration frequencies ( $\text{cm}^{-1}$ ) are obtained as: 3633 (O–H), 3038 (Ar–C–H), 1240 (C–O), 1586 (C=N), 1459 (N=N), 1066 (N–O).

These frequencies and their experimental values are subjected to linear regression analysis. Correlation constant of this analysis is found as 0.9913. According to this result, there is a good agreement between experimental and calculated frequencies.

#### The local reactivity

The active center of deprotonated tautomer (**1a**) can be determined by using local softness and Fukui functions of atoms in molecule. Deprotonated form of tautomer (**1a**) is optimized at B3LYP/6-31++G(d,p) level in gas phase. Local softness ( $s$ ) and nucleophilic attack ( $f_k^+$ ) which is the Fukui function are calculated with Eqs. (1) and (2) [42,43].

$$s = \frac{2}{(E_{\text{LUMO}} - E_{\text{HOMO}})} \times [P_k(N) - P_k(N - 1)] \quad (1)$$

$$f_k^+ = P_k(N + 1) - P_k(N) \quad (2)$$

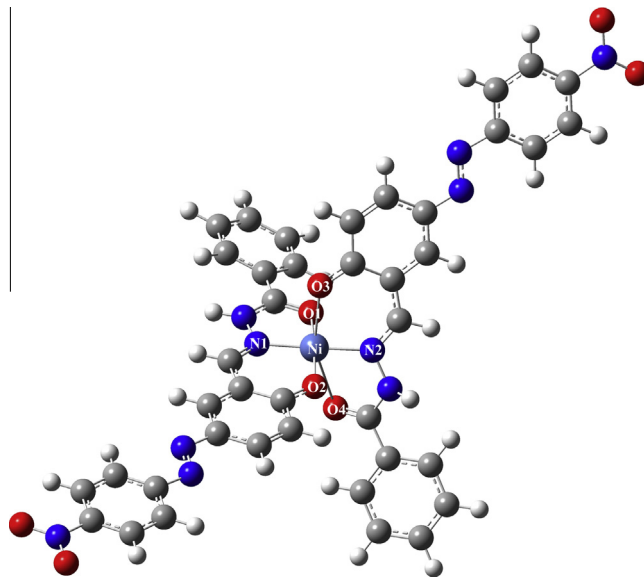


Fig. 8. Optimized structure of  $[\text{Ni}(\text{sb})_2]$  complex at B3LYP/LANL2DZ level in gas phase.

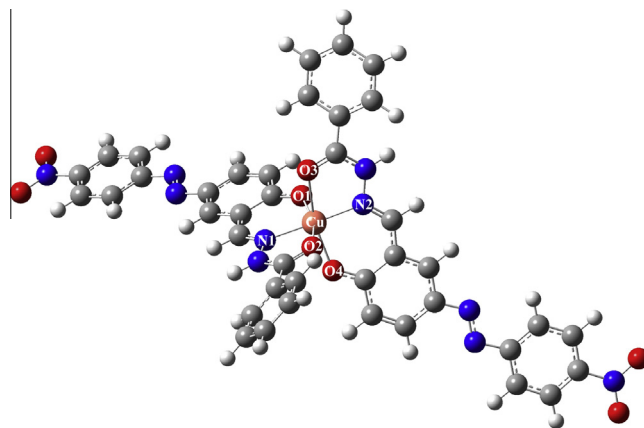


Fig. 9. Optimized structure of  $[\text{Cu}(\text{sb})_2]$  complex at B3LYP/LANL2DZ level in gas phase.

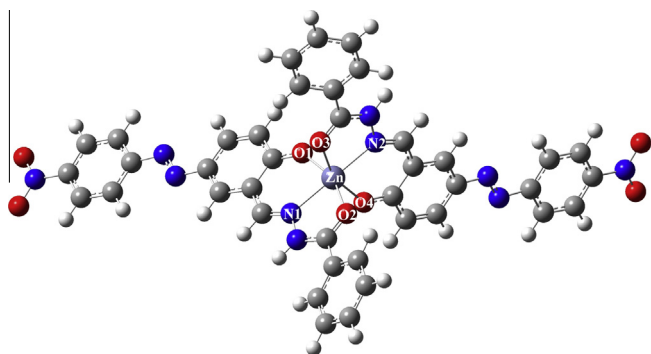


Fig. 10. Optimized structure of [Zn(sb)<sub>2</sub>] complex at B3LYP/LANL2DZ level in gas phase.

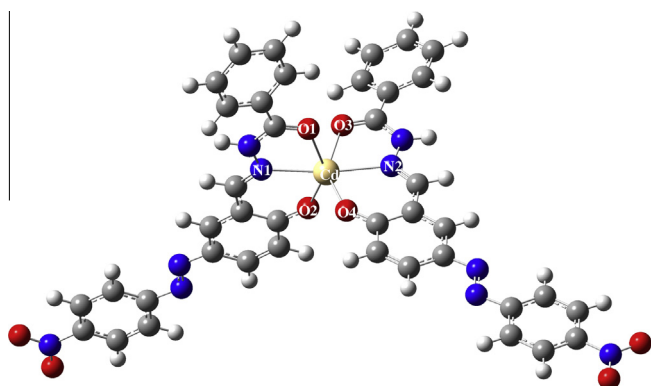


Fig. 11. Optimized structure of [Cd(sb)<sub>2</sub>] complex at B3LYP/LANL2DZ level in gas phase.

where  $P_k(N+1)$ ,  $P_k(N)$  and  $P_k(N-1)$  are the charges of the atoms on the systems with  $N+1$ ,  $N$ ,  $N-1$  electrons.  $E_{\text{HOMO}}$  and  $E_{\text{LUMO}}$  are the highest occupied molecular orbital energy and the lowest unoccupied molecular orbital energy, respectively. The  $P_k(N+1)$ ,

Table 6

Calculated vibration frequencies ( $\text{cm}^{-1}$ ) at B3LYP/LANL2DZ level at gas phase and correlation constant ( $R^2$ ) values.

	$V_{\text{C-H (Arom.)}}$	$V_{\text{C=N}}$	$V_{\text{N=N}}$	$V_{\text{N-O}}$	$V_{\text{M-O}}$	$V_{\text{M-O}}$	$R^2$
[Co(sb) <sub>2</sub> ]	3107	1583	1343	1080	664	516	0.9941
[Ni(sb) <sub>2</sub> ]	31145	1552	1439	1080	662	520	0.9993
[Cu(sb) <sub>2</sub> ]	3093	1531	1442	1080	749	519	0.9994
[Zn(sb) <sub>2</sub> ]	3094	1528	1423	1080	644	545	0.9988
[Cd(sb) <sub>2</sub> ]	3107	1528	1448	1080	642	542	0.9995

$P_k(N)$ ,  $P_k(N-1)$ , Fukui function for nucleophilic attack and local softness are given in Table 4 for some donor atoms in tautomer (1a).

There are many donor atoms in tautomer (1a). This tautomer is three-dentate ligand that is proven experimentally in this study. Fukui function and local softness can be used for determining the most active atom towards metal atoms. According to the  $f_k^+$  and  $s$ , the most active atom is O2 atom ( $f_k^+ = -0.39204$  and  $s = 0.14531$ ). Therefore, tautomer (1a) uses the O2 atom when bonding with metal. After that, coordinate-covalent bond is formed between N2 and metal. If the bonding is formed from O3 or O4 atom, structure of complex will be very strained. Therefore, metal prefers the bonding from N2 atom. Finally, the bond is formed between metal and O1. This evaluation is proven by using Fukui functions and local softness.

Molecular electrostatic potential (MEP) diagram for deprotonated form of tautomer (1) is mapped up at the level of B3LYP/LANL2DZ theory with optimized geometry. The MEP diagram of tautomer (1a) is represented in Fig. 6. The positive (blue) and negative (red) regions of MEP are related to electrophilic and nucleophilic reactivity, respectively. In the MEP diagram of deprotonated form of tautomer (1a), the most negative regions are represented as zones 1, 2 and 3. In zones 1 and 2, the negative regions are mainly localized on oxygen atoms. As for the zone 3, nitrogen atom is activated by  $\pi$  electrons.

#### The optimized structures and vibration frequencies of complexes

Optimized structures of [Co(sb)<sub>2</sub>]-4H<sub>2</sub>O, [Ni(sb)<sub>2</sub>]-H<sub>2</sub>O, [Cu(sb)<sub>2</sub>]-4H<sub>2</sub>O, [Zn(sb)<sub>2</sub>]-H<sub>2</sub>O and [Cd(sb)<sub>2</sub>]-H<sub>2</sub>O are calculated at B3LYP/LANL2DZ level in gas phase and given in Figs. 7–11,

Table 5

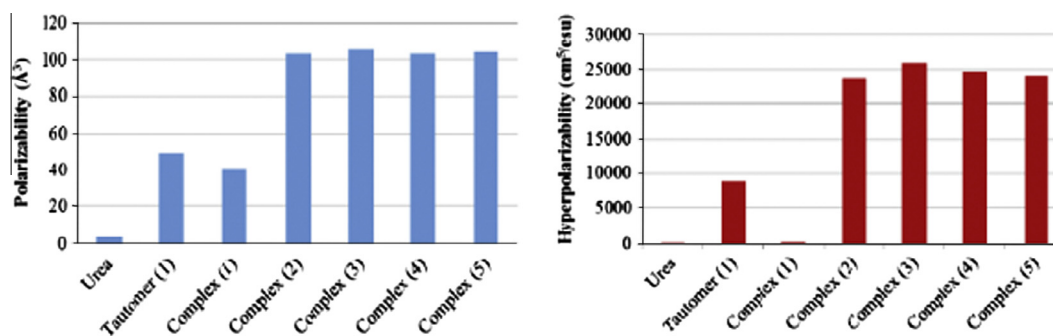
Calculated geometrical parameters of relevant complexes at B3LYP/LANL2DZ level.

Bond lengths (Å)	[Co(sb) <sub>2</sub> ]-4H <sub>2</sub> O	[Ni(sb) <sub>2</sub> ]-H <sub>2</sub> O	[Cu(sb) <sub>2</sub> ]-4H <sub>2</sub> O	[Zn(sb) <sub>2</sub> ]-H <sub>2</sub> O	[Cd(sb) <sub>2</sub> ]-H <sub>2</sub> O
M–N1	1.932	1.904	1.991	2.187	2.407
M–N2	1.913	1.884	1.988	2.186	2.406
M–O1	2.217	2.318	2.278	2.198	2.353
M–O2	2.071	2.680	2.067	2.030	2.207
M–O3	1.966	1.964	2.063	2.028	2.206
M–O4	2.069	1.876	2.275	2.199	2.355
Bond Angles (deg.)					
N1–M–N2	177.4	176.4	176.5	173.4	172.2
N1–M–O1	79.9	88.4	77.6	74.1	68.9
N1–M–O2	91.1	72.0	89.4	83.6	77.1
N1–M–O3	89.7	93.0	92.6	100.7	107.9
N1–M–O4	95.8	89.5	99.8	101.0	105.4
N2–M–O1	98.6	91.7	99.8	101.0	105.2
N2–M–O2	90.2	107.2	92.7	100.6	108.0
N2–M–O3	92.4	83.4	89.5	83.6	77.1
N2–M–O4	81.9	93.7	77.6	74.1	68.9
O1–M–O2	170.0	157.0	163.4	156.4	145.4
O1–M–O3	88.4	82.3	86.0	90.9	93.7
O1–M–O4	88.8	104.2	86.5	86.7	90.0
O2–M–O3	96.0	86.8	105.2	100.5	102.8
O2–M–O4	87.8	87.9	85.5	90.5	93.0
O3–M–O4	173.2	173.1	163.8	156.7	145.5

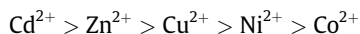
M: Metal atom.

**Table 7**The calculated dipole moment ( $\mu$ ), polarizability ( $\alpha$ ) and hyperpolarizability ( $\beta$ ) for tautomer (1a) and mentioned complexes.

	Tautomer (1a)	[Co(sb) <sub>2</sub> ] <sub>2</sub> (1)	[Ni(sb) <sub>2</sub> ] <sub>2</sub> (2)	[Cu(sb) <sub>2</sub> ] <sub>2</sub> (3)	[Zn(sb) <sub>2</sub> ] <sub>2</sub> (4)	[Cd(sb) <sub>2</sub> ] <sub>2</sub> (5)
$\mu_x^a$	2.5241	-0.4626	-1.8366	-0.0501	-0.0971	-0.0658
$\mu_y^a$	0.8945	-0.6936	4.7695	6.5039	7.6533	7.4593
$\mu_z^a$	0.1052	0.5520	1.6661	-0.0188	-0.0683	-0.06278
$\alpha_{xx}^b$	578.6714	422.2826	1556.5790	1414.8938	1294.3750	1334.3890
$\alpha_{yy}^b$	37.1451	11.6574	-0.8052	11.8583	10.6425	11.8295
$\alpha_{zz}^b$	391.4924	398.8246	539.6064	713.5822	788.8305	768.3616
$\alpha_{xy}^b$	-9.4018	33.8563	24.6240	6.6718	22.9897	40.9989
$\alpha_{xz}^b$	-6.6612	6.0494	-7.0106	-10.9065	-7.8733	-6.7427
$\alpha_{yz}^b$	151.3945	425.2902	591.1687	582.0254	544.5088	546.2184
$\beta_{xxx}^b$	-7997.9198	-235.8349	1906.2346	-484.7714	-351.7793	-420.2525
$\beta_{yyy}^b$	-4802.7735	212.1989	-24436.9930	-29182.4491	-27187.5160	-26289.1500
$\beta_{zzz}^b$	-2406.7417	147.6071	-1499.4045	84.4034	185.8050	250.0008
$\beta_{xxy}^b$	-503.3435	185.0239	-673.3176	-4081.5522	-2678.5204	-1046.5988
$\beta_{xxy}^b$	-158.4538	69.2882	-3605.4751	-127.5076	-277.3544	-305.6399
$\beta_{xzz}^b$	-52.2101	10.0966	3874.3861	4.914.8745	4645.1822	4268.1874
$\beta_{xzz}^b$	-37.0283	103.4493	-800.4356	83.9897	-5.2386	26.2933
$\beta_{yzz}^b$	28.8360	42.1253	970.4951	141.0069	-36.2375	-72.7850
$\beta_{yyz}^b$	13.7035	-73.7760	804.0116	1117.5799	2550.7871	2899.2310
$\mu^a$	2.6800	0.9999	5.3757	6.5042	7.6543	7.4599
$\alpha^c$	49.7589	41.1343	103.5010	105.7215	103.4253	104.4493
$\beta^d$	$8.78 \times 10^{-26}$	$2.92 \times 10^{-27}$	$2.36 \times 10^{-25}$	$2.60 \times 10^{-25}$	$2.47 \times 10^{-25}$	$2.40 \times 10^{-25}$

<sup>a</sup> In Debye.<sup>b</sup> In atomic unit (a.u.).<sup>c</sup> In Å<sup>3</sup>.<sup>d</sup> In cm<sup>5</sup>/esu.**Fig. 12.** The graphs of polarizability and hyperpolarizability for the mentioned compounds and urea.

respectively. Calculated structural parameters of mentioned complexes are given in Table 5. According to Table 5, there are six bonds around the metal atoms. As theoretically, the radii of metal ions decrease as follows in strong field:



Electron density around the nucleus is the maximum in Cd<sup>2+</sup> ion while is the minimum in Co<sup>2+</sup> ion. Therefore, bond lengths mainly increase with increasing the radii of metal ions. The same bond lengths and angle values are mainly similar in each complex.

No imaginary frequencies were found in calculations for relevant complexes. Calculated vibration frequencies and correlation constants ( $R^2$ ) between calculated and experimental frequencies are given in Table 6. There is a good correlation between experimental frequencies and their calculated results.

#### The non-linear optical properties

Non-linear optical properties (NLO) are current research field because of its importance in providing the key functions of frequency shifting, optical modulation, optical switching, optical logic and optical memory. Therefore, the NLO properties play an important role for design of materials in communication technology and

optical devices [44]. The NLO properties increase with conjugation of  $\pi$  electrons or adding donor/acceptor groups to molecule. Polarizability ( $\alpha$ ) and hyperpolarizability ( $\beta$ ) can be used to describe the relationship between the electronic structures of molecules and their NLO properties. The polarizability and hyperpolarizability increase with increasing the delocalization of  $\pi$  electrons. Therefore, the NLO properties increase with increasing polarizability and hyperpolarizability. NLO properties of tautomer (1) and mentioned complexes are studied with DFT/B3LYP method.

The total static dipole moment ( $\mu$ ), the average linear polarizability ( $\alpha$ ) and first hyperpolarizability ( $\beta$ ) are calculated by using Eqs. (3)–(5), respectively [44].

$$\mu = \sqrt{\mu_x^2 + \mu_y^2 + \mu_z^2} \quad (3)$$

$$\alpha = \frac{1}{3}(\alpha_{xx} + \alpha_{yy} + \alpha_{zz}) \quad (4)$$

$$\beta = [(\beta_{xxx} + \beta_{yyy} + \beta_{zzz})^2 + (\beta_{xxy} + \beta_{xyx} + \beta_{yzz})^2 + (\beta_{zzz} + \beta_{xxx} + \beta_{yyy})^2]^{1/2} \quad (5)$$

Calculated polarizability and hyperpolarizability of mentioned compounds were presented in Table 7. In many theoretical studies, urea is taken into account as reference substance. The polarizability and

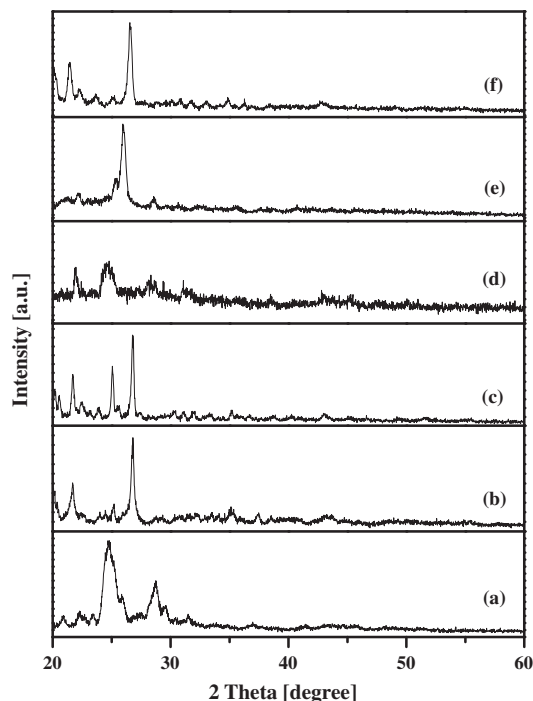


**Fig. 13.** The XRD diffraction patterns of (a)  $\text{sbH}\cdot\text{H}_2\text{O}$ , (b)  $[\text{Cd}(\text{sb})_2]\cdot\text{H}_2\text{O}$ , (c)  $[\text{Co}(\text{sb})_2]\cdot 4\text{H}_2\text{O}$ , (d)  $[\text{Cu}(\text{sb})_2]\cdot 4\text{H}_2\text{O}$ , (e)  $[\text{Ni}(\text{sb})_2]\cdot\text{H}_2\text{O}$  and (f)  $[\text{Zn}(\text{sb})_2]\cdot\text{H}_2\text{O}$ .

hyperpolarizability values of this substance are equal to  $3.8312 \text{ \AA}^3$  and  $0.37289 \times 10^{-30} \text{ cm}^5/\text{esu}$ , respectively [45]. The polarizability and hyperpolarizability values of mentioned compounds and reference substance are plotted in Fig. 12. According to Fig. 12, the polarizability and hyperpolarizability of tautomer (**1a**) and complexes are greater than urea. This result means that tautomer (**1a**) and mentioned complexes have NLO properties. The polarizability and hyperpolarizability of complex 3, which is  $[\text{Cu}(\text{sb})_2]$ , are higher than the others. Therefore, this complex has the most effective NLO properties.

**Table 8**  
XRD data of the  $[\text{Cd}(\text{sb})_2]\cdot\text{H}_2\text{O}$  metal complex.

P. no.	<i>h</i>	<i>k</i>	<i>l</i>	2Th.(o) (°)	2Th.(c) (°)	d-sp.(o) (Å)	d-sp.(c) (Å)	Rel. Int. (%)
1	2	0	0	11.8411	11.8325	7.467796	7.473225	21.12
2	1	1	0	13.2269	13.2404	6.688346	6.681538	20.74
3	2	0	1	14.9159	14.8879	5.93459	5.945692	9.77
4	1	1	-1	15.508	15.5282	5.709305	5.701929	27.6
5	0	0	2	16.8243	16.8389	5.265467	5.260922	13.54
6	2	1	-1	18.4958	18.4929	4.793204	4.793962	19.93
7	2	0	-2	20.1332	20.1028	4.406921	4.413511	32.01
8	1	1	2	21.6945	21.73	4.093177	4.086568	48.52
9	3	1	-1	22.6532	22.6904	3.922064	3.915726	6.55
10	3	0	-2	23.9359	23.9193	3.714706	3.717257	7.32
11	1	2	0	24.4977	24.549	3.630775	3.623313	10.77
12	3	0	2	25.1893	25.2428	3.532636	3.525276	19.38
13	3	1	-2	26.8453	26.7667	3.318366	3.327921	100
14	2	0	3	28.6629	28.6609	3.111933	3.112142	4.9
15	5	0	-1	30.6289	30.6295	2.916511	2.91646	4.74
16	5	0	1	31.5143	31.5184	2.836566	2.836208	4.79
17	5	1	0	32.2777	32.2288	2.771194	2.775292	6.7
18	5	0	-2	33.5577	33.6616	2.668363	2.660365	5.54
19	3	2	-2	34.0413	34.0001	2.631551	2.634648	4.22
20	0	2	-3	35.0579	35.0705	2.557538	2.556646	10.42
21	4	2	-2	37.492	37.4907	2.396895	2.396981	11.11
22	5	2	0	38.5216	38.5454	2.335171	2.33378	6.37
23	6	1	-2	41.0501	41.0425	2.196981	2.197372	3.4
24	4	0	4	43.0674	43.0561	2.098629	2.099154	7.13
25	8	0	0	48.6957	48.6986	1.86841	1.868306	1.47
26	8	2	-1	55.2202	55.2061	1.662089	1.66248	1.75

### X-ray powder diffraction analysis

Growth of single crystals of azo–azomethine compounds failed, so they were characterized by XRD [46,47]. X-ray powder diffraction analysis of the sbH ligand and its metal complexes was carried out to understand the type of crystal system, lattice parameters and the cell volume. As shown in Fig. 13 the XRD patterns indicate crystalline nature for the sbH ligand and its metal complexes. Indexing of the diffraction patterns were performed using HighScore Plus software. For example, for the Cd(II) and Ni(II) complexes, their Miller indices (*h k l*) along with observed and calculated  $2\theta$  angles, *d* values and relative intensities were given in Tables 8 and 9. Also, from the indexed data the unit cell parameters were calculated and listed in Table 10. The powder XRD patterns of the compounds are completely different from those of the starting materials, demonstrating the formation of coordination compounds. It is found that sbH ligand, Cd(II), and Zn(II) complexes have monoclinic structure, while Co(II), Cu(II), and Ni(II) complexes have orthorhombic structure. The crystal structures of similar type of samples were reported as monoclinic and orthorhombic [48,49]. Also, in order to investigate the crystalline information of the all samples, the crystallite sizes *D* were calculated from the most intense peaks using Sherrer's formula [50]. The calculated results are given in Table 10.

### Ames mutagenicity test results

sbH·H<sub>2</sub>O, the presence and absence of metabolic activation system for mutagenic strains TA98, while TA100 strain in the same medium did not show such an effect.  $[\text{Cu}(\text{sb})_2]\cdot 4\text{H}_2\text{O}$ , the presence and absence of metabolic activation system for TA98 strain showed a strong mutagenic effect, in the same environment. TA100 strain showed the highest concentration of a mutagenicity.  $[\text{Ni}(\text{sb})_2]\cdot\text{H}_2\text{O}$ , the presence and absence of metabolic activation system for TA98 strain showed a strong mutagenic effects, TA100 strains only at the highest concentration in the presence of metabolic systems has shown mutagenic effects. Moreover, the presence and absence of metabolic system TA98 strain revertants dose-dependently

**Table 9**  
XRD data of the  $[\text{Ni}(\text{sb})_2]\cdot\text{H}_2\text{O}$  metal complex.

P. no.	<i>h</i>	<i>k</i>	<i>l</i>	2Th.(o) (°)	2Th.(c) (°)	d-sp.(o) (Å)	d-sp.(c) (Å)	Rel. Int. (%)
1	0	1	0	10.5948	10.5278	8.343335	8.396242	16.89
2	1	1	0	12.5023	12.516	7.074296	7.066612	13.36
3	0	0	2	14.9573	15.0712	5.918257	5.873757	53.78
4	1	0	2	16.5643	16.5297	5.347516	5.358649	10.94
5	2	1	0	17.2678	17.168	5.131216	5.160823	32.5
6	0	1	2	18.4672	18.4193	4.800557	4.812942	22.83
7	0	2	0	21.1189	21.1458	4.203414	4.198121	6.41
8	1	2	0	22.1933	22.2206	4.002285	3.997433	10.79
9	3	1	0	23.0139	22.9581	3.861404	3.870655	3.57
10	3	0	2	25.402	25.4145	3.503536	3.501848	30.23
11	1	1	3	25.9504	25.9936	3.430729	3.425126	100
12	2	1	3	28.5993	28.5919	3.118707	3.119501	9.94
13	3	0	3	30.7165	30.6575	2.908392	2.913863	2.73
14	3	1	3	32.4683	32.4994	2.755362	2.752802	2.8
15	0	3	2	35.5084	35.5015	2.526113	2.526591	3.33
16	5	0	2	37.5697	37.5957	2.392119	2.390527	3.01
17	2	0	5	40.7798	40.7734	2.21092	2.211248	4.18

**Table 10**  
XRD parameters of the sbH ligand and its metal complexes.

Sample	Lattice parameters				Volume (Å <sup>3</sup> )	Crystallite size <i>D</i> (nm)	Crystal system
	<i>a</i> (Å)	<i>b</i> (Å)	<i>c</i> (Å)	$\beta$ (°)			
(1) (sbH·H <sub>2</sub> O)	20.0986	4.8815	16.0517	121.2430	1346.46	36	Monoclinic
(2) [Co(sb) <sub>2</sub> ] <sub>2</sub> ·4H <sub>2</sub> O	22.6700	10.3893	8.2069	90	1932.94	49	Orthorhombic
(3) [Ni(sb) <sub>2</sub> ] <sub>2</sub> ·H <sub>2</sub> O	13.0821	8.4076	11.7446	90	1291.77	93	Orthorhombic
(4) [Cu(sb) <sub>2</sub> ] <sub>2</sub> ·4H <sub>2</sub> O	12.2197	10.8324	5.7546	90	761.73	27	Orthorhombic
(5) [Zn(sb) <sub>2</sub> ] <sub>2</sub> ·H <sub>2</sub> O	13.9605	14.8258	8.9747	121.7830	1579	93	Monoclinic
(6) [Cd(sb) <sub>2</sub> ] <sub>2</sub> ·H <sub>2</sub> O	14.9687	7.4861	10.5176	92.9437	1177.02	118	Monoclinic

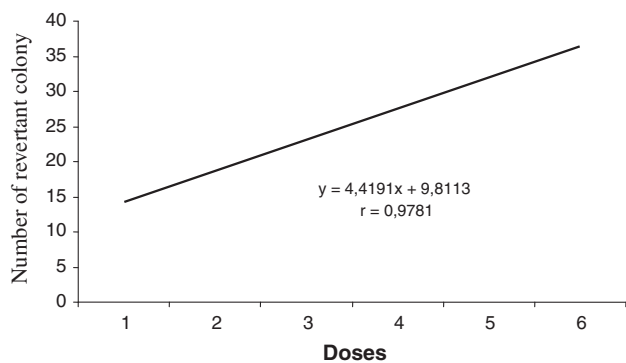


**Fig. 14.** Dose-dependently increase in the mutagenic activity of  $[\text{Ni}(\text{sb})_2]\cdot\text{H}_2\text{O}$  on TA98 strain in the absence of metabolic activation system.

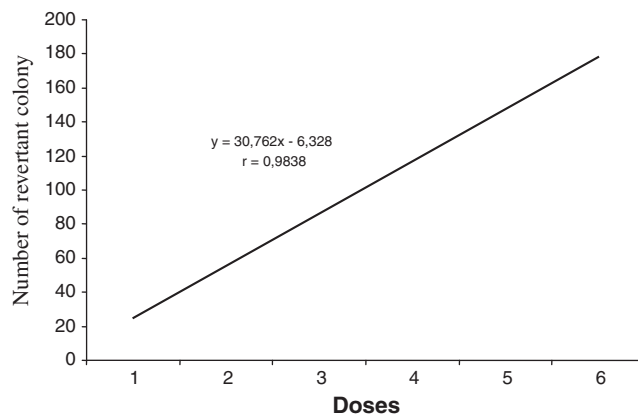


**Fig. 16.** Dose-dependently increase in the mutagenic activity of  $[\text{Co}(\text{sb})_2]\cdot 4\text{H}_2\text{O}$  on TA98 strain in the presence of metabolic activation system.

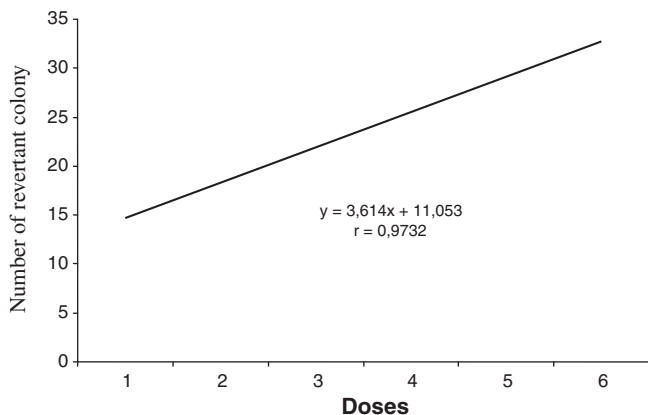


**Fig. 15.** Dose-dependently increase in the mutagenic activity of  $[\text{Ni}(\text{sb})_2]\cdot\text{H}_2\text{O}$  on TA98 strain in the presence of metabolic activation system.

increased the percentage of colonies (Fig. 14,  $r = 0.9781$ ; Fig. 15,  $r = 0.9732$ ).

$[\text{Co}(\text{sb})_2]\cdot 4\text{H}_2\text{O}$ , in the presence of metabolic activation system and in the absence, both in TA98 and TA100 strain showed very strong mutagenic effects. On the other hand in the presence of S9 TA98 strain number of revertants dose-dependently increased the number of colonies (Fig. 16,  $r = 0.9732$ ).

$[\text{Zn}(\text{sb})_2]\cdot\text{H}_2\text{O}$ , in the presence of metabolic activation system for TA100 strains did not show any mutagenic effect, strain TA98 in the absence of the metabolic systems has shown mutagenic effects.  $[\text{Cd}(\text{sb})_2]\cdot\text{H}_2\text{O}$ , in the presence and absence of metabolic activation system for TA98 strain showed weak mutagenic activity, TA100 strain did not show any mutagenic activity (Table 11).

**Table 11**The mutagenicity of ligand and its metal complexes in *Salmonella typhimurium* TA98 and TA100 strains in the absence (-S9) or presence (+S9) of S9 mix.

Test substances	Concentrat.mg/plate	TA98		TA100	
		-S9	+S9	-S9	+S9
Spontaneous control	-	11.67 ± 2.51	12.50 ± 1.93	106.7 ± 12.9	103.00 ± 9.57
NPD	200 µg/ml	3025 ± 172			
2-AF	20 µg/ml		3510 ± 247		743.2 ± 38.2
SA	1 µg/ml			651.8 ± 48.5	
sbH-H <sub>2</sub> O	0.80	31.00 ± 2.84***	22.73 ± 1.65***	95.5 ± 11.6	123.8 ± 14.7
	0.40	31.67 ± 4.23**	26.17 ± 4.74*	86.33 ± 4.07*	121.5 ± 10.02
	0.20	31.67 ± 4.23**	24.33 ± 3.62*	92.17 ± 7.23	104.79 ± 4.67
	0.10	23.33 ± 3.03*	14.69 ± 3.02	79.17 ± 4.56**	99.3 ± 9.4
	0.05	25.67 ± 2.29**	15.67 ± 3.51	51.83 ± 7.90***	61.52 ± 4.90***
[Cu(sb) <sub>2</sub> ]-4H <sub>2</sub> O	0.80	227.2 ± 43.6***	63.6 ± 10.3**	421.2 ± 83.5***	273.9 ± 52.9**
	0.40	190.5 ± 41.8***	71.68 ± 8.07***	322.5 ± 61.2***	211.4 ± 48.3*
	0.20	141.2 ± 18.0***	64.0 ± 11.9**	231.8 ± 57.9*	123.8 ± 17.5
	0.10	118.83 ± 6.04***	56.00 ± 6.67***	237.3 ± 37.3**	103.50 ± 9.36
	0.05	129.3 ± 21.1***	41.67 ± 6.59*	133.7 ± 16.0	84.79 ± 7.45
[Ni(sb) <sub>2</sub> ]-H <sub>2</sub> O	0.80	34.67 ± 2.29***	32.67 ± 4.27***	168.0 ± 12.5**	120.09 ± 8.73
	0.40	32.50 ± 6.41***	28.17 ± 3.42***	144.7 ± 16.0	102.32 ± 8.19
	0.20	28.00 ± 3.62***	25.00 ± 2.83***	108.3 ± 24.9	94.3 ± 11.20
	0.10	24.33 ± 1.20***	23.87 ± 1.67***	98.8 ± 16.9	96.5 ± 13.4
	0.05	20.50 ± 2.57*	20.00 ± 3.09	89.17 ± 4.68*	79.2 ± 15.7
[Co(sb) <sub>2</sub> ]-4H <sub>2</sub> O	0.80	26.50 ± 2.47**	171.0 ± 16.7***	28.83 ± 3.05**	475.2 ± 96.0**
	0.40	29.67 ± 2.58***	143.5 ± 13.4***	31.33 ± 4.12**	490.5 ± 92.6***
	0.20	27.67 ± 2.87**	132.2 ± 18.7**	28.17 ± 2.90**	249.0 ± 32.6**
	0.10	22.67 ± 2.16**	84.0 ± 12.9**	23.00 ± 2.07**	199.6 ± 22.7*
	0.05	20.50 ± 2.88*	64.84 ± 5.42***	17.83 ± 1.99*	132.5 ± 13.9
[Zn(sb) <sub>2</sub> ]-H <sub>2</sub> O	0.80	27.33 ± 3.19**	14.57 ± 2.54	129.00 ± 4.14**	51.93 ± 4.90***
	0.40	30.17 ± 1.85***	14.16 ± 1.92	134.00 ± 7.82*	49.17 ± 7.05**
	0.20	21.50 ± 1.84**	13.34 ± 3.35	117.8 ± 11.9	33.81 ± 4.80***
	0.10	15.83 ± 3.35	8.19 ± 1.32*	108.33 ± 9.08	27.50 ± 2.78***
	0.05	14.50 ± 1.61	6.57 ± 3.29*	78.83 ± 6.18**	39.2 ± 16.4**
[Cd(sb) <sub>2</sub> ]-H <sub>2</sub> O	0.80	36.33 ± 1.78***	36.83 ± 2.33***	121.17 ± 6.32	106.00 ± 7.35
	0.40	28.33 ± 5.17*	31.67 ± 4.60**	90.33 ± 3.99*	95.17 ± 7.11
	0.20	15.33 ± 1.23*	21.33 ± 2.70*	93.50 ± 7.98	93.17 ± 5.51
	0.10	19.33 ± 2.54*	19.00 ± 1.81**	74.0 ± 10.3*	76.50 ± 5.79*
	0.05	14.33 ± 3.28	15.00 ± 2.37	59.00 ± 5.99***	67.2 ± 10.9*

NPD: 4-nitro-o-phenylenediamine, 2AF: 2-Aminoflourene, SA: Sodium azid.

\* P &lt; 0.05.

\*\* P &lt; 0.01.

\*\*\* P &lt; 0.001.

## Conclusion

In this work, azo (—N=N—) and nitro (—NO<sub>2</sub>) chromophore groups containing azo-azomethine ligand, *N'*-[2-hydroxy-5-[(4-nitrophenyl)diazanyl]phenyl] methylidene]benzohydrazidemonohydrate, (sbH-H<sub>2</sub>O) derived from 2-hydroxy-5-[(4-nitrophenyl)diazanyl]benzaldehyde with benzohydrazide in EtOH and its some transition metal chelates have been synthesized. The analytical data and the spectroscopic studies suggested that the complexes had general formula of [M(sb)<sub>2</sub>]-nH<sub>2</sub>O, where M is cobalt(II), nickel(II), copper(II), zinc(II) or cadmium(II) ions. According to the UV-Vis. and IR data of the nitrophenylazo linked Schiff base ligand, sbH-H<sub>2</sub>O was coordinated to the metal ion through the azomethine nitrogen (—CH=N—) and oxygen atoms of the hydroxyl (—OH) and carbonyl (C=O) groups. From the XRD results, it is found that mbH ligand, Cd(II), and Zn(II) complexes have monoclinic structure, while Co(II), Cu(II), and Ni(II) complexes have orthorhombic structure. Based on the above results, the structure of the coordination compounds under investigation can be formulated. All in all, except for [Zn(sb)<sub>2</sub>]-H<sub>2</sub>O complex, ligand and the metal complexes in the presence and absence of metabolic activation system to the TA98 strain have been found to show mutagenic activity. [Zn(sb)<sub>2</sub>]-H<sub>2</sub>O complex only in the absence of metabolic activation system has shown mutagenic activity.

On the other hand [Cu(sb)<sub>2</sub>]-4H<sub>2</sub>O and [Co(sb)<sub>2</sub>]-4H<sub>2</sub>O metal complexes in the presence and absence of metabolic activation system for TA100 strains have shown mutagenic activity, the ligand and its metal complexes, statistically not significantly increased. This situation [Cu(sb)<sub>2</sub>]-4H<sub>2</sub>O and [Co(sb)<sub>2</sub>]-4H<sub>2</sub>O metal complexes and their metabolites induce point mutations the other complexes and the ligand did not show such activity (Table 11).

## Acknowledgement

This work was financially supported by the Unit of Coordination of Scientific Research Projects, Kahramanmaraş Sütçü İmam University, Kahramanmaraş, Turkey (Project no: 2010/2-15YLS). Also, the authors wish to thank Prof. Dr. Vickie McKee, Department of Chemistry at Loughbrough University, Leicestershire, UK for <sup>1</sup>H NMR measurements.

## References

- [1] Z.H. Chohan, S.K.A. Sheazi, *Synth. React. Inorg. Met.-Org. Chem.* 29 (1999) 105–118.
- [2] N. Dharmaraj, P. Viswanalhamurthi, K. Natarajan, *Transition Met. Chem.* 26 (2001) 105–109.
- [3] C.H. Collins, P.M. Lyne, *Microhiul Methods*, University Park Press, Baltimore, 1970, p. 422.
- [4] D. Chen, A.E. Martell, *Inorg. Chem.* 26 (1987) 1026–1030.

- [5] S. Badiger, R.S. Hunoor, B.R. Patil, R.S. Vadavi, C.V. Mangannavar, I.S. Muchchandi, Y.P. Patil, M. Nethaji, K.B. Gudasi, *Inorg. Chim. Acta* 384 (2012) 197–203.
- [6] C.M. Metzler, A. Cahill, D.E. Metzler, *J. Am. Chem. Soc.* 102 (1980) 6075–6082.
- [7] A. Ray, S. Banerjee, G.M. Rosair, V. Gramlich, S. Mitra, *Struct. Chem.* 19 (2008) 459–465.
- [8] P. Vicini, F. Zani, P. Cozzini, I. Doytchinova, *Eur. J. Med. Chem.* 37 (2002) 553–564.
- [9] C. Loncle, J.M. Brunel, N. Vidal, M. Dherbomez, Y. Letourneux, *Eur. J. Med. Chem.* 39 (2004) 1067–1071.
- [10] B.K. Kaymakcioglu, S. Rollas, *Farmaco* 57 (2002) 595–599.
- [11] J. Patole, D. Shingapurkar, S. Padhye, C. Ratledge, *Bioorg. Med. Chem. Lett.* 16 (2006) 1514–1517.
- [12] O.A. El-Gammal, G.A. El-Reash, S.F. Ahmed, *J. Mol. Struct.* 1007 (2012) 1–10.
- [13] S. Rollas, S.G. Kucukguzel, *Molecules* 12 (2007) 1910–1938.
- [14] P. Vicini, M. Incerti, I.A. Doytchinova, P. La Colla, B. Busonera, R. Loddò, *Eur. J. Med. Chem.* 41 (2006) 624–632.
- [15] H.J.C. Bezerra-Netto, D.I. Lacerda, A.L.P. Miranda, H.M. Alves, E.J. Barreiro, C.A.M. Fraga, *Bioorg. Med. Chem.* 14 (2006) 7924–7935.
- [16] a) G.A. Al-Hazmi, A.A. El-Asmy, *J. Coord. Chem.* 62 (2009) 337–345;  
b) L.H. Abdel-Rahman, R.M. El-Khatib, L.A.E. Nassr, A.M. Abu-Dief, *J. Mol. Struct.* 1040 (2013) 9–18;  
c) L.H. Abdel-Rahman, R.M. El-Khatib, L.A.E. Nassr, A.M. Abu-Dief, M. Ismail, A.A. Seleem, *Spectrochim. Acta* 117 (2014) 366–378.
- [17] M. Bakir, I. Hassan, J. Johnson, O. Brown, O. Green, C. Gyles, M.D. Coley, *J. Mol. Struct.* 688 (2004) 213–222.
- [18] B. Cabir, B. Avar, M. Gulcan, A. Kayraldiz, M. Kurtoglu, *Turk. J. Chem.* 37 (2013) 422–438.
- [19] M. Aslantas, N. Kurtoglu, E. Sahin, M. Kurtoglu, *Acta Cryst. E* 634 (2007) o3637.
- [20] M. Köse, N. Kurtoğlu, Ö. Gümüşsu, D. Karakaş, M. Tutak, V. McKee, M. Kurtoğlu, *J. Mol. Struct.* 1053 (2013) 89.
- [21] GaussView 5.0, Gaussian Inc., Wallingford, CT, USA, 2009.
- [22] Gaussian 09, AM64L-Revision-C.01, Gaussian Inc., Wallingford, CT, USA, 2010.
- [23] R. Ramaekers, J. Pajak, M. Rospenk, G. Maes, *Spectrochim. Acta Part A* 61 (2005) 1347–1356.
- [24] Y. Zhang, X. Zhang, Z. Liu, H. Xu, J. Jiang, *Vib. Spectrosc.* 40 (2006) 289–298.
- [25] K. Mortelmans, E. Zeiger, *Mutat. Res.* 455 (2000) 29–60.
- [26] D.M. Maron, B.N. Ames, *Mutat. Res.* 113 (1983) 173–215.
- [27] D. Krewski, B.G. Leroux, S.R. Bleuer, L.H. Broekhoeve, *Biometrics* 49 (1993) 499–510.
- [28] A. Kayraldiz, F.F. Kaya, S. Canimoğlu, E. Rencüzoğulları, *Ann. Microbiol.* 56 (2006) 129–133.
- [29] Z.H. Chohan, M. Hanif, *Appl. Organomet. Chem.* 25 (2011) 753–760.
- [30] M. Robert, *Spectroscopic Identification of Organic Compounds*, Silverstein, seventh ed., John Wiley & Sons, 2005. p. 104.
- [31] A.A.A. Aziz, A.N.M. Salem, M.A. Sayed, M.M. Aboaly, *J. Mol. Struct.* 1010 (2012) 130–138.
- [32] N. Deligonul, M. Tumer, S. Serin, *Transition Met. Chem.* 31 (2006) 920–929.
- [33] H.E. Gottlieb, V. Kotlyar, A. Nudelman, *J. Org. Chem.* 62 (1997) 7512–7515.
- [34] I.S. Ahmed, M.M. Moustafa, M.M. Abd El Aziz, *Spectrochim. Acta Part A* 78 (2011) 1429–1436.
- [35] N.M. Shuaib, N.A. Al-Awadi, A. El-Dissouky, A.G. Shoair, *J. Coord. Chem.* 59 (2006) 743–757.
- [36] I.S. Ahmed, M.A. Kassem, *Spectrochim. Acta Part A* 77 (2010) 359–366.
- [37] S.M. Ben-Saber, A.A. Maihub, S.S. Hudere, M.M. El-Ajaily, *Microchem. J.* 81 (2005) 191–194.
- [38] M. Kurtoglu, F. Purtaş, S. Toroglu, *Transition Met. Chem.* 33 (2008) 705–710.
- [39] E. Ispir, *Dyes Pigments* 82 (2009) 13–19.
- [40] S.A. Shaker, H. Khaledi, H.M. Ali, *Chem. Papers* 65 (2011) 299–307.
- [41] R. Kilincarslan, E. Erdem, H. Kocaokutgen, *Transition Met. Chem.* 32 (2007) 102–106.
- [42] M.M. Kabanda, L.C. Murulana, E.E. Ebenso, *Int. J. Electrochem. Sci.* 7 (2012) 7179–7205.
- [43] M. Torrent-Sucarrat, F. De Proft, P. Geerlings, P.W. Ayers, *Chem. Eur. J.* 14 (2008) 8652–8660.
- [44] D. Sajan, J. Hubert, V.S. Jayakumar, J. Zaleski, *J. Mol. Struct.* 785 (2006) 43–53.
- [45] M. Arivazhagan, R. Kavitha, V.P. Subhasini, *Spectrochim. Acta Part A* 128 (2014) 701–710.
- [46] S.S. Chavan, V.A. Sawant, *J. Mol. Struct.* 965 (2010) 1–6.
- [47] M. Bal, G. Ceyhan, B. Avar, M. Kose, A. Kayraldiz, M. Kurtoğlu, *Turk. J. Chem.* 38 (2014) 222–241.
- [48] S.M. Jadhav, A.S. Munde, S.G. Shankarwar, V.R. Patharkar, V.A. Shelke, T.K. Chondhekar, *J. Korean Chem. Soc.* 54 (2010) 515–522.
- [49] M. Mirzaei, H. Aghabozorg, H. Eshtiagh-Hosseini, *J. Iran Chem. Soc.* 8 (2011) 580–607.
- [50] B.D. Cullity, *Elements of X-ray diffraction*, Addison Wesley, London, 1978. p. 101.